

Theory of Photolonization Threshold Spectroscopy of Molecules and Clusters

S. H. Lin,

Department of Chemistry, Arizona State University, Tempe, Arizona 85287

H. L. Selzle, K. O. Börnsen, and E. W. Schlag*

Institute for Physical and Theoretical Chemistry, Technical University of Munich,
8046 Garching, West Germany (Received: July 27, 1987; In Final Form: October 14, 1987)

In this paper we have developed a theoretical treatment of photoionization threshold spectroscopy (PITS) of molecules, van der Waals complexes (or clusters), and hydrogen-bonding systems. We have treated the thermal PITS, single vibronic level PITS, and microcanonical PITS. Some numerical results are presented to demonstrate the application of theoretical results. We have also analyzed the PITS of benzene dimer.

1. Introduction

Recently it has been well demonstrated that two-color resonance-enhanced multiphoton ionization (MPI) spectroscopy is a very useful technique in studying the ionic states and high excited states of molecules or clusters.^{1–6} In two-color MPI experiments, ionization of a molecule is accomplished with two lasers by making use of a resonance intermediate state; the first laser is used to excite the molecule to a specific vibronic (or rovibronic) level in its first excited electronic state and the second laser is used to scan across the ionization threshold. The ionization potential is determined by the onset of the ion current. This technique leads to a direct and accurate determination of the ionization potentials of molecules.

It is known that the ionization potential of a molecule decreases in going from the gas to the solution and the magnitude of the decrease amounts to 1–3 eV.⁷ It has been found that the ionization potential of a weak complex (like a van der Waals complex or hydrogen-bonding complex) or cluster is always smaller than that of the free molecule and depends on the size of the complex or cluster. It has also been found that, for a weak complex or cluster, in the ionization threshold region the photoionization spectrum often exhibits structures or long tails.^{8–13} The tail can be as long as 2000–3000 cm⁻¹. It is the purpose of this paper to report the theoretical investigation of this photoionization threshold

spectroscopy (PITS). The qualitative aspect of the results in the present paper is probably known to many workers; they are concerned with the behavior of the photoionization cross sections of molecules and weak complexes (or clusters) in the neighborhood of the threshold.^{14,15} It is believed, however, that the generality and applicability of the theoretical results to be presented in this paper have not been emphasized before, nor have they been derived with the same claim for general validity as will be done in the present paper. To demonstrate the application, we shall also apply the theoretical results to analyze our PITS data of (benzene)₂.

2. Theory

In previous papers,¹⁶ the density matrix method (or generalized master equation approach) has been applied to study one-photon photoionization and two-color two-photon photoionization of molecules. Effect of autoionization states on photoionization has been studied. We have shown that in the weak field case and without the presence of autoionization states, the rate constant for photoionization from the vibronic (or rovibronic) level (*iv*) to the ionic vibronic (or rovibronic) level (*kv*) can be expressed as^{16,17}

$$R_{kv} = (2\pi/\hbar) \sum_k |\langle \tilde{k}v | \hat{D} | iv \rangle|^2 \delta(\hbar\omega - E_{kv} + E_{iv}) \quad (2-1)$$

where \tilde{k} denotes the wave vector of the photoelectron. The single vibronic (or rovibronic) level rate constant for photoionization is the sum over all final vibronic states

$$R_v = \sum_{v'} R_{kv'} = (2\pi/\hbar) \sum_{v'} \sum_k |\langle \tilde{k}v | \hat{D} | iv \rangle|^2 \delta(\hbar\omega - E_{kv'} + E_{iv}) \quad (2-2)$$

and the thermal average rate constant for photoionization is the sum over all the final vibronic states and thermally averaged over all the initial vibronic states, i.e.

$$R = \sum_v \sum_{v'} P_{iv} R_{kv'} = (2\pi/\hbar) \sum_v \sum_{v'} P_{iv} |\langle \tilde{k}v | \hat{D} | iv \rangle|^2 \delta(\hbar\omega - E_{kv'} + E_{iv}) \quad (2-3)$$

where P_{iv} denotes the Boltzmann factor. Equations 2-1–2-3 are for photoelectron spectroscopy.

For the photoionization efficiency experiment, we perform the integration over the kinetic energy of photoelectron in (2-1)–(2-3). Corresponding to R_{kv} we now have

(14) Wigner, E. P. *Phys. Rev.* **1948**, *73*, 1002.(15) Guyon, P. M.; Berkowitz, J. J. *Chem. Phys.* **1971**, *54*, 1814. Berkowitz, J. *Photoabsorption, Photoionization and Photoelectron Spectroscopy*; Academic: New York, 1979.(16) Boeglin, A.; Fain, B.; Lin, S. H. *J. Chem. Phys.* **1986**, *84*, 4838. Fain, B.; Kono, H.; Lin, S. H.; Henke, W. E.; Selzle, H. L.; Schlag, E. W. *J. Chin. Chem. Soc. (Taipei)* **1985**, *32*, 187 (invited paper).(17) Sobolewski, A. L.; Domcke, W. *J. Chem. Phys.* **1987**, *86*, 176.(1) Ito, M.; Fujii, M. *Advances in Multiphoton Processes and Spectroscopy*, in press.(2) Börnsen, K. O.; Selzle, H. L.; Schlag, E. W. *J. Chem. Phys.* **1986**, *85*, 1726. Fung, K. H.; Henke, W. E.; Hays, T. R.; Selzle, H. L.; Schlag, E. W. *J. Phys. Chem.* **1981**, *85*, 3560.(3) Reisler, H.; Wittig, C. *Adv. Chem. Phys.* **1985**, *60*, 1. Kimura, K. *Adv. Chem. Phys.* **1985**, *60*, 161.(4) Nasona, Y.; Achiba, Y.; Kimura, K. *J. Chem. Phys.* **1986**, *84*, 1063. Nasona, Y.; Achiba, Y.; Kimura, K. *J. Phys. Chem.* **1986**, *90*, 1288.(5) Carrasquillo, E.; Zwier, T. S.; Levy, D. H. *J. Chem. Phys.* **1986**, *83*, 4990.(6) Castleman, A. W., Jr.; Keese, R. G. *Acc. Chem. Res.* **1986**, *19*, 413.(7) Yakolev, B. S.; Lukin, L. V. *Adv. Chem. Phys.* **1985**, *60*, 99.(8) Law, K. S.; Schauer, M.; Bernstein, E. R. *J. Chem. Phys.* **1984**, *81*, 4871. Law, K. S.; Schauer, M.; Bernstein, E. R. *J. Chem. Phys.* **1985**, *82*, 3722. Law, K. S.; Schauer, M.; Bernstein, E. R. *J. Chem. Phys.* **1985**, *82*, 736.(9) Rühl, E.; Bisling, P. G. F.; Brutschy, B.; Baumgärtel, H. *Chem. Phys. Lett.* **1986**, *126*, 232.(10) Fuke, K.; Yoshiuchi, H.; Kaya, K.; Achiba, Y.; Sata, K.; Kimura, K. *Chem. Phys. Lett.* **1984**, *108*, 179. Castella, M.; Tramer, A.; Piuze, F. *Chem. Phys. Lett.* **1986**, *129*, 105.(11) Gonohe, N.; Abe, H.; Mikami, N.; Ito, M. *J. Phys. Chem.* **1985**, *89*, 3642. Gonohe, N.; Shimizu, A.; Abe, H.; Mikami, N.; Ito, M. *Chem. Phys. Lett.* **1984**, *107*, 22.(12) Williamson, A. D.; Compton, R. N.; Eland, J. H. D. *J. Chem. Phys.* **1979**, *70*, 590.(13) Hager, J.; Ivanco, M.; Smith, M. A.; Wallace, S. C. *Chem. Phys.* **1986**, *105*, 397.

$$G_{vv'}(\omega) = (2\pi/\hbar) |\langle \tilde{k}v | \hat{D} | iv \rangle|^2 H(\hbar\omega - I - E_{v'} + E_v) \quad (2-4)$$

where $H(x)$ represents the Heaviside function (i.e., $H(x) = 1$ for $x \geq 0$ and $H(x) = 0$ for $x < 0$). I is the ionization potential, and $E_{v'}$ and E_v denote the vibrational (or rovibrational) energy of the ion and the initial electronic state, respectively. For simplicity the molecular rotation will be ignored, but it can be included easily. Similarly for the single vibronic level case and the thermal average case, we find

$$G_v(E) = (2\pi/\hbar) \sum_{v'} |\langle \tilde{k}v | \hat{D} | iv \rangle|^2 H(E - I - E_{v'} + E_v) \quad (2-5)$$

and

$$G(E) = (2\pi/\hbar) \sum_v \sum_{v'} P_{iv} |\langle \tilde{k}v | \hat{D} | iv \rangle|^2 H(E - I - E_{v'} + E_v) \quad (2-6)$$

where $E = \hbar\omega$. Using the adiabatic approximation and Condon approximation (i.e., for allowed transitions), we obtain

$$|\langle \tilde{k}v | \hat{D} | iv \rangle|^2 = |D_{ki}|^2 |\langle v | v \rangle|^2 \quad (2-7)$$

where $|\langle v | v \rangle|^2$ denotes the Franck-Condon factor and $D_{ki} = -(1/2) \tilde{E}_0 \langle k | \tilde{\mu} | i \rangle$. The factor $|D_{ki}|^2$ does not vary much over the photon energy considered here (i.e., in the ionization threshold region) and will be assumed to be constant.¹⁷

From (2-1)–(2-3) we can see that the photoionization photoelectron spectrum consists of a series of δ functions (or Lorentzians) weighted by the Franck-Condon factor; from (2-4)–(2-6), we can see that the photoionization efficiency spectrum consists of a series of step functions weighted by the Franck-Condon factor.

In the gas phase where collision between molecules is significant, the red-shift in the photoionization threshold spectra is observed and is often attributed to the ionization of the excited Rydberg states induced by collision.¹² However, from (2-6) we can see that the thermal population of vibrational excited states can also cause the red-shift in the photoionization threshold spectra.

In the case of a weak complex or cluster, because of low-frequency modes introduced in the process of forming the complex or cluster, the photoionization threshold spectra are changed because of the Franck-Condon factors of these low-frequency modes. In other words, from the analysis of the photoionization threshold spectroscopy it may be possible to obtain some information about the structure changes in the ionization.

A. Thermal Average Case. To find the expression for analyzing the photoionization threshold spectra, we first consider the thermal average case. Applying the Laplace transformation to (2-6) yields¹⁸

$$L[G(E)] = \int_0^\infty dE \exp(-\beta E) G(E) = (2\pi/\beta\hbar) |D_{ki}|^2 \sum_v \sum_{v'} P_{iv} |\langle v | v \rangle|^2 \exp[-\beta(I + E_{v'} - E_v)] \quad (2-8)$$

Here the relation given by (2-7) has been used. L represents the Laplace transformation operator. In the harmonic oscillator case, we can rewrite (2-8) as

$$L[G(E)] = (2\pi/\beta\hbar) |D_{ki}|^2 e^{-\beta I} \prod_j F_j(\beta) \quad (2-9)$$

where

$$F_j(\beta) = \sum_{v_j} \sum_{v'_j} P_{iv_j} |\langle v_j | v'_j \rangle|^2 \exp[-\beta(E_{v'_j} - E_{v_j})] \quad (2-10)$$

From (2-9) we can see that $G(E)$ can be obtained by performing the inverse Laplace transformation

$$G(E) = \frac{2\pi}{\hbar} |D_{ki}|^2 \frac{1}{2\pi i} \int_c \frac{d\beta}{\beta} \exp[\beta(E - I)] \prod_j F_j(\beta) \quad (2-11)$$

In other words, the central problem involved in the calculation of photoionization threshold spectra is the evaluation of $F_j(\beta)$ and the contour integral appearing in the inverse Laplace transform.

$F_j(\beta)$ can be evaluated by using Mehler's formula (or Slater sum). For the displaced-oscillator case, we obtain (Appendix A)

$$F_j(\beta) = \exp \left[-S_j \left\{ \coth \frac{\hbar\omega_j}{2kT} - \operatorname{csch} \frac{\hbar\omega_j}{2kT} \cosh \left(\frac{\hbar\omega_j}{2kT} - \beta\hbar\omega_j \right) \right\} \right] \quad (2-12)$$

where T is the temperature of the system and S_j represents the coupling constant of the j th vibrational mode (related to the dimensionless vibrational coordinate displacement between the two electronic states). $F_j(\beta)$ for a displaced-distorted oscillator is given in Appendix A.

Substituting (2-12) into (2-11) yields

$$G(E) = \frac{2\pi}{\hbar} |D_{ki}|^2 \frac{1}{2\pi i} \int_c \frac{d\beta}{\beta} \exp \left[\beta(E - I) - \sum_j S_j \left\{ \coth \frac{\hbar\omega_j}{2kT} - \operatorname{csch} \frac{\hbar\omega_j}{2kT} \cosh \left(\frac{\hbar\omega_j}{2kT} - \beta\hbar\omega_j \right) \right\} \right] \quad (2-13)$$

Notice that at $T = 0$ we have

$$F_j(\beta) = \exp[-S_j(1 - e^{-\beta\hbar\omega_j})] \quad (2-14)$$

and

$$G_0(E) = \frac{2\pi}{\hbar} |D_{ki}|^2 \frac{1}{2\pi i} \int_c \frac{d\beta}{\beta} \exp[\beta(E - I) - \sum_j S_j(1 - e^{-\beta\hbar\omega_j})] \quad (2-15)$$

Now it is important to find a good approximation method to evaluate the contour integral involved in (2-13) or (2-15); an exact evaluation of this contour integral will only lead the expression of $G(E)$ back to that given by (2-6). It should be noted that the contour integral involved in (2-13) or (2-15) for photoionization threshold spectroscopy is similar to that in the expressions for rate constant of radiationless transitions, absorption coefficient of molecular electronic spectra, molecular electronic emission spectra, etc., and that this type of contour integral can be integrated approximately by using the saddle-point method (or the method of steepest descent).¹⁸

Applying the saddle-point method to (2-13), we obtain

$$G(E) = \frac{2\pi}{\hbar} |D_{ki}|^2 \left\{ \left[\exp \left[\beta^*(E - I) - \sum_j S_j \left(\coth \frac{\hbar\omega_j}{2kT} - \operatorname{csch} \frac{\hbar\omega_j}{2kT} \cosh \left(\frac{\hbar\omega_j}{2kT} - \beta^*\hbar\omega_j \right) \right) \right] \right] / \left[2\pi \left\{ 1 + \sum_j S_j (\beta^*\hbar\omega_j) \operatorname{csch} \frac{\hbar\omega_j}{2kT} \cosh \left(\frac{\hbar\omega_j}{2kT} - \beta^*\hbar\omega_j \right) \right\} \right]^{1/2} \right\} \quad (2-16)$$

where β^* represents the saddle-point value of β and is to be determined from

$$E - I = \frac{1}{\beta^*} + \sum_j (S_j \hbar\omega_j) \operatorname{csch} \frac{\hbar\omega_j}{2kT} \sinh \left(\frac{\hbar\omega_j}{2kT} - \beta^* \hbar\omega_j \right) \quad (2-17)$$

At $T = 0$, (2-16) and (2-17) reduce to

$$G_0(E) = \frac{2\pi}{\hbar} |D_{ki}|^2 \frac{\exp[\beta^*(E - I) - \sum_j S_j(1 - e^{-\beta^*\hbar\omega_j})]}{[2\pi \{1 + \sum_j S_j (\beta^*\hbar\omega_j)^2 e^{-\beta^*\hbar\omega_j}\}]^{1/2}} \quad (2-18)$$

and

$$E - I = 1/\beta^* + \sum_j (S_j \hbar\omega_j) e^{-\beta^*\hbar\omega_j} \quad (2-19)$$

respectively. From (2-16) or (2-18), we can see that, to construct a photoionization threshold spectrum, we first choose a frequency

(18) Eyring, H.; Lin, S. H.; Lin, S. M. *Basic Chemical Kinetics*; Wiley-Interscience: New York, 1980; Chapters 5 and 7.

ω (i.e., $E = \hbar\omega$) and then calculate the saddle-point value β^* from (2-17) (or 2-19); substituting this β^* value into (2-16) (or (2-18)), we can evaluate $G(E)$. This process should be repeated for each ω value.

B. Single Vibronic Level Case. Applying the Laplace transformation to $G_v(E)$ given by (2-5) we obtain

$$L[G_v(E)] = \frac{2\pi}{\beta\hbar} |D_{kl}|^2 \exp[-\beta(I - E_v)] \prod_j F_{v_j}(\beta) \quad (2-20)$$

where

$$F_{v_j}(\beta) = \sum_{v_j'} \langle v_j' | v_j \rangle^2 \exp(-\beta E_{v_j'}) \quad (2-21)$$

The evaluation of $F_{v_j}(\beta)$ is more complicated; the result for a displaced oscillator is given by (Appendix B)

$$F_{v_j}(\beta) = \exp[-(v_j + 1/2)\beta\hbar\omega_j - S_j(1 - e^{-\beta\hbar\omega_j})] \sum_{n_j=0}^{v_j} \frac{v_j!}{n_j![(v_j - n_j)!]^2} \left(4S_j \sinh^2 \frac{\beta\hbar\omega_j}{2} \right)^{v_j - n_j} \quad (2-22)$$

The expression of $F_{v_j}(\beta)$ for a displaced-distorted oscillator is derived in Appendix B. Substituting (2-22) into (2-20) yields

$$L[G_v(E)] = \frac{2\pi}{\beta\hbar} |D_{kl}|^2 \exp[-\beta I - \sum_j S_j(1 - e^{-\beta\hbar\omega_j})] \prod_j \left\{ \sum_{n_j=0}^{v_j} \frac{v_j!}{n_j![(v_j - n_j)!]^2} \left(S_j \sinh^2 \frac{\beta\hbar\omega_j}{2} \right)^{v_j - n_j} \right\} \quad (2-23)$$

and

$$G_v(E) = \frac{2\pi}{\hbar} |D_{kl}|^2 \left(\frac{1}{2\pi i} \right) \int_c \frac{d\beta}{\beta} \exp[\beta(E - I) - \sum_j S_j(1 - e^{-\beta\hbar\omega_j})] \times \prod_j \left\{ \sum_{n_j=0}^{v_j} \frac{v_j!}{n_j![(v_j - n_j)!]^2} \left(S_j \sinh^2 \frac{\beta\hbar\omega_j}{2} \right)^{v_j - n_j} \right\} \quad (2-24)$$

Again the saddle-point method can be used to evaluate the contour integral in (2-24); we find

$$G_v(E) = G_0(E) \prod_j \left\{ \sum_{n_j=0}^{v_j} \frac{v_j!}{n_j![(v_j - n_j)!]^2} \left(S_j \sinh^2 \frac{\beta^* \hbar \omega_j}{2} \right)^{v_j - n_j} \right\} \quad (2-25)$$

where $G_0(E)$ is given by (2-18) and the saddle-point value β^* is given by (2-19).

3. Duschinsky Effect

In the photoionization of dimers or hydrogen-bonding systems, the Duschinsky effect may be very important due to the fact that the structures of ions and neutral species may be quite different. To treat this effect, we shall study a coupled two-mode case. The multidimensional Franck-Condon integral with the Duschinsky mixing effect has recently been studied by Kupka and Cribb.¹⁹

For the thermal average PITS, we have to evaluate (see (2-6), (2-7), and (2-9))

$$F(\beta) = \sum_{v'} \sum_{v''} P_{iv} |\langle v' | v \rangle|^2 e^{-\beta(E_{v'} - E_v)} \quad (3-1)$$

Notice that if the potential surface of the initial electronic state is described by

$$V_i = \frac{1}{2} \omega_1^2 Q_1^2 + \frac{1}{2} \omega_2^2 Q_2^2 \quad (3-2)$$

then the potential surface of the ionic state can be represented by

$$V_k = V_k^0 + \frac{1}{2} \omega_1'^2 Q_1'^2 + \frac{1}{2} \omega_2'^2 Q_2'^2 + \alpha Q_1 Q_2 + a_1 Q_1 + a_2 Q_2 \quad (3-3)$$

to take into account of frequency changes ($\omega_i \neq \omega_i'$), mode mixing ($\alpha \neq 0$), and normal coordinate displacements ($a_i \neq 0$). We shall diagonalize the V_k surface by introducing new coordinates (Q_1' , Q_2') as

$$Q_1 = \sin \theta Q_1' + \cos \theta Q_2' + d_1 \quad (3-4)$$

and

$$Q_2 = -\cos \theta Q_1' + \sin \theta Q_2' + d_2 \quad (3-5)$$

That is

$$V_k = V_{k0} + \frac{1}{2} \omega_1''^2 Q_1'^2 + \frac{1}{2} \omega_2''^2 Q_2'^2 \quad (3-6)$$

where

$$V_{k0} = V_k^0 + \frac{1}{2} \omega_1'^2 d_1^2 + \frac{1}{2} \omega_2'^2 d_2^2 + a_1 d_1 + a_2 d_2 \quad (3-7)$$

$$\tan 2\theta = 2\alpha / (\omega_1'^2 - \omega_2'^2) \quad (3-8)$$

$$d_1 = (a_2 \alpha - a_1 \omega_2'^2) / (\omega_1'^2 \omega_2'^2 - \alpha^2) \quad (3-9)$$

$$d_2 = (a_1 \alpha - a_2 \omega_1'^2) / (\omega_1'^2 \omega_2'^2 - \alpha^2) \quad (3-10)$$

$$\omega_1''^2 = \omega_1'^2 \sin^2 \theta + \omega_2'^2 \cos^2 \theta - \alpha \sin 2\theta \quad (3-11)$$

and

$$\omega_2''^2 = \omega_1'^2 \cos^2 \theta + \omega_2'^2 \sin^2 \theta + \alpha \sin 2\theta \quad (3-12)$$

In other words, we determine θ by using (3-8) and (d_1 , d_2) by using (3-9) and (3-10).

The thermal distribution function for PITS can formally be written as

$$F(\beta) = \sum_{v'} \sum_{v''} P_{iv} e^{-\beta(E_{v'} - E_v)} \int_{-\infty}^{\infty} \int_{-\infty}^{\infty} dQ' dQ'' X_{v'}(Q') X_{v''}(Q'') X_v(Q) X_v(Q'') \quad (3-13)$$

where $dQ' = dQ_1' dQ_2'$, $X_v = X_{v1} X_{v2}$, etc. Applying the Slater sum to (3-13), we obtain

$$F(\beta) = \left[\prod_{i=1}^2 \frac{\beta_i \beta_i''}{Q_i(T) (4\pi^2 \sin \beta \hbar \omega_i'' \sinh \beta' \hbar \omega_i)^{1/2}} \right] \times \int_{-\infty}^{\infty} \int_{-\infty}^{\infty} dQ' dQ'' \exp \left[-\sum_{i=1}^2 \frac{\beta_i'^2}{4} \left\{ (Q_i' + \bar{Q}_i'')^2 \tanh \frac{\beta \hbar \omega_i''}{2} + (Q_i' - \bar{Q}_i'')^2 \coth \frac{\beta \hbar \omega_i''}{2} \right\} - \sum_{i=1}^2 \frac{\beta_i^2}{4} \left\{ (Q_i + \bar{Q}_i)^2 \tanh \frac{\beta' \hbar \omega_i}{2} + (Q_i - \bar{Q}_i)^2 \coth \frac{\beta' \hbar \omega_i}{2} \right\} \right] \quad (3-14)$$

where $\beta' = 1/kT - \beta$, $\beta_i = (\omega_i/\hbar)^{1/2}$, and $Q_i(T)$ represents the partition function

$$Q_i(T) = e^{-\hbar \omega_i / 2kT} / (1 - e^{-\hbar \omega_i / kT}) = \left(2 \sinh \frac{\hbar \omega_i}{2kT} \right)^{-1} \quad (3-15)$$

Substituting (3-4) and (3-5) into (3-14) yields

$$F(\beta) = K(\beta) \int_{-\infty}^{\infty} \int_{-\infty}^{\infty} dQ' dQ'' \exp[-a_{11}'(Q_1' + \bar{Q}_1'')^2 - a_{22}'(Q_2' + \bar{Q}_2'')^2 - 2a_{12}'(Q_1' + \bar{Q}_1'')(Q_2' + \bar{Q}_2'') - a_{11}''(Q_1' - \bar{Q}_1'')^2 - a_{22}''(Q_2' - \bar{Q}_2'')^2 - 2a_{12}''(Q_1' - \bar{Q}_1'')(Q_2' - \bar{Q}_2'')] \quad (3-16)$$

(19) Kupka, H.; Cribb, P. H. *J. Chem. Phys.* **1986**, *85*, 1303.

(20) DeVault, D. *Quantum-Mechanical Tunneling in Biological Systems*; Cambridge University Press: Cambridge, U.K., 1985. Lin, S. H. *J. Chem. Phys.* **1966**, *44*, 3759.

where

$K(\beta) =$

$$\prod_i \frac{\beta_i \beta_i'' \sinh \frac{\hbar \omega_i}{2kT}}{(\pi^2 \sinh \beta \hbar \omega_i'' \sinh \beta' \hbar \omega_i)^{1/2}} \exp\left(-\beta_i^2 d_i^2 \tanh \frac{\beta' \hbar \omega_i}{2}\right) \quad (3-17)$$

$$a_{11}' = \frac{1}{4} \left(\beta_1''^2 \tanh \frac{\beta \hbar \omega_1''}{2} + \beta_1^2 \sin^2 \theta \tanh \frac{\beta' \hbar \omega_1}{2} + \beta_2^2 \cos^2 \theta \tanh \frac{\beta' \hbar \omega_2}{2} \right) \quad (3-18)$$

$$a_{22}' = \frac{1}{4} \left(\beta_2''^2 \tanh \frac{\beta \hbar \omega_2''}{2} + \beta_1^2 \cos^2 \theta \tanh \frac{\beta' \hbar \omega_1}{2} + \beta_2^2 \sin^2 \theta \tanh \frac{\beta' \hbar \omega_2}{2} \right) \quad (3-19)$$

$$2a_{12}' = \frac{1}{4} \sin 2\theta \left(\beta_1^2 \tanh \frac{\beta' \hbar \omega_1}{2} - \beta_2^2 \tanh \frac{\beta' \hbar \omega_2}{2} \right) \quad (3-20)$$

$$c_{11} = \frac{1}{4} \left(\beta_1''^2 \coth \frac{\beta \hbar \omega_1''}{2} + \beta_1^2 \sin^2 \theta \coth \frac{\beta' \hbar \omega_1}{2} + \beta_2^2 \cos^2 \theta \coth \frac{\beta' \hbar \omega_2}{2} \right) \quad (3-21)$$

$$c_{22} = \frac{1}{4} \left(\beta_1''^2 \coth \frac{\beta \hbar \omega_2''}{2} + \beta_1^2 \cos^2 \theta \coth \frac{\beta' \hbar \omega_1}{2} + \beta_2^2 \sin^2 \theta \coth \frac{\beta' \hbar \omega_2}{2} \right) \quad (3-22)$$

$$2c_{12} = \frac{1}{4} \sin 2\theta \left(\beta_1^2 \coth \frac{\beta' \hbar \omega_1}{2} - \beta_2^2 \coth \frac{\beta' \hbar \omega_2}{2} \right) \quad (3-23)$$

$$a_{11}' = \beta_1^2 d_1 \sin \theta \tanh \frac{\beta' \hbar \omega_1}{2} - \beta_2^2 d_2 \cos \theta \tanh \frac{\beta' \hbar \omega_2}{2} \quad (3-24)$$

and

$$a_{21}' = \beta_1^2 d_1 \cos \theta \tanh \frac{\beta' \hbar \omega_1}{2} + \beta_2^2 d_2 \sin \theta \tanh \frac{\beta' \hbar \omega_2}{2} \quad (3-25)$$

To perform the integrations in (3-16) we introduce the new variables

$$x_1 = Q_1' + \bar{Q}_1', \quad y_1 = Q_1' - \bar{Q}_1' \quad (3-26)$$

$$x_2 = Q_2' + \bar{Q}_2', \quad y_2 = Q_2' - \bar{Q}_2' \quad (3-27)$$

to rewrite $F(\beta)$ as

$F(\beta) =$

$$(K(\beta)/4) \int_{-\infty}^{\infty} \int_{-\infty}^{\infty} dx_1 dy_1 \int_{-\infty}^{\infty} \int_{-\infty}^{\infty} dx_2 dy_2 \exp(-a_{11}' x_1^2 - a_{22}' x_2^2 - 2a_{12}' x_1 x_2 - a_1' x_1 - a_2' x_2 - c_{11} y_1^2 - c_{22} y_2^2 - 2c_{12} y_1 y_2) \quad (3-28)$$

The off-diagonal terms can be eliminated by rotating the coordinate systems

$$y_1 = \sin \theta_1 y_1' + \cos \theta_1 y_2'; \quad y_2 = -\cos \theta_1 y_1' + \sin \theta_1 y_2' \quad (3-29)$$

$$x_1 = \sin \theta_2 x_1' + \cos \theta_2 x_2'; \quad x_2 = -\cos \theta_2 x_1' + \sin \theta_2 x_2' \quad (3-30)$$

It follows that

$F(\beta) = (K(\beta)/4) \times$

$$\int_{-\infty}^{\infty} \int_{-\infty}^{\infty} dx_1' dx_2' \int_{-\infty}^{\infty} \int_{-\infty}^{\infty} dy_1' dy_2' \exp(-a_{11}'' x_1'^2 - a_{22}'' x_2'^2 - a_1'' x_1' - a_2'' x_2' - c_{11}' y_1'^2 - c_{22}' y_2'^2) \quad (3-31)$$

or

$F(\beta) =$

$$(K(\beta)/4) \left(\frac{\pi^4}{a_{11}'' a_{22}'' c_{11}' c_{22}'} \right)^{1/2} \exp\left(\frac{a_1''^2}{4a_{11}''} + \frac{a_2''^2}{4a_{22}''} \right) \quad (3-32)$$

where

$$c_{11}' = c_{11} \sin^2 \theta_1 + c_{22} \cos^2 \theta_1 - a_{12} \sin 2\theta_1 \quad (3-33)$$

$$c_{22}' = c_{11} \cos^2 \theta_1 + c_{22} \sin^2 \theta_1 + a_{12} \sin 2\theta_1 \quad (3-34)$$

$$\tan 2\theta_1 = 2c_{12}/(c_{11} - c_{22}) \quad (3-35)$$

$$a_{11}'' = a_{11}' \sin^2 \theta_2 + a_{22}' \cos^2 \theta_2 - a_{12}' \sin 2\theta_2 \quad (3-36)$$

$$a_{22}'' = a_{11}' \cos^2 \theta_2 + a_{22}' \sin^2 \theta_2 + a_{12}' \sin 2\theta_2 \quad (3-37)$$

$$\tan 2\theta_2 = 2a_{12}'/(a_{11}' - a_{22}') \quad (3-38)$$

$$a_1'' = a_1' \sin \theta_2 - a_2' \cos \theta_2 \quad (3-39)$$

and

$$a_2'' = a_1' \cos \theta_2 + a_2' \sin \theta_2 \quad (3-40)$$

Substituting (3-17) into (3-32) we obtain

$$F(\beta) = \prod_{j=1}^2 \frac{\beta_j \beta_j'' \sinh \frac{\hbar \omega_j}{2kT}}{2(a_{jj}'' c_{jj}' \sinh \beta \hbar \omega_j'' \sinh \beta' \hbar \omega_j)^{1/2}} \exp\left(\frac{a_j''^2}{4a_{jj}''} - \beta_j^2 d_j^2 \tanh \frac{\beta' \hbar \omega_j}{2} \right) \quad (3-41)$$

4. Discussion

We shall first present some numerical results to demonstrate the theoretical results given in the previous section. For this purpose, we introduce an average frequency $\bar{\omega}$ for ω_j 's. In this case, (2-16) can be written as

$$G(E_r) = \frac{\exp\left[\beta_r^* E_r - S \left(\coth \frac{1}{2T_r} - \operatorname{csch} \frac{1}{2T_r} \cosh \left(\frac{1}{2T_r} - \beta_r^* \right) \right) \right]}{\left[2\pi \left\{ 1 + S \beta_r^{*2} \operatorname{csch} \frac{1}{2T_r} \cosh \left(\frac{1}{2T_r} - \beta_r^* \right) \right\} \right]^{1/2}} \quad (4-1)$$

where

$$E_r = \frac{1}{\beta_r^*} + S \operatorname{csch} \frac{1}{2T_r} \sinh \left(\frac{1}{2T_r} - \beta_r^* \right) \quad (4-2)$$

Here the reduced quantities are defined as

$$G(E)_r = \frac{G(E)}{\frac{2\pi}{\hbar} |D_{kl}|^2} \quad (4-3)$$

$$E_r = \frac{E - I}{\hbar \bar{\omega}}; \quad \beta_r = \beta \hbar \bar{\omega}; \quad T_r = \frac{kT}{\hbar \bar{\omega}}; \quad S = \sum_j S_j \quad (4-4)$$

Equations 4-1 and 4-2 can also be applied to the single-mode case.

In Figures 1-4 we show the calculated photoionization threshold spectra using (4-1). The exact calculated spectra are also shown for comparison. As can be seen from these figures, the computed spectra by using the saddle-point method are in excellent agreement with the exact spectra. It should be noted that the saddle-point method is simply to provide a good approximation method to convert the step-function curves into the smooth ones.

From Figures 1-4, we can see that the tail of PITS increases with increasing S values, and for the strong coupling case (see, for example, the $S = 10$ case), the determination of the ionization threshold by visual observation will in general lead to an overestimate of the ionization energy. In other words, in this case a fitting of the PITS curve is necessary in order to determine the

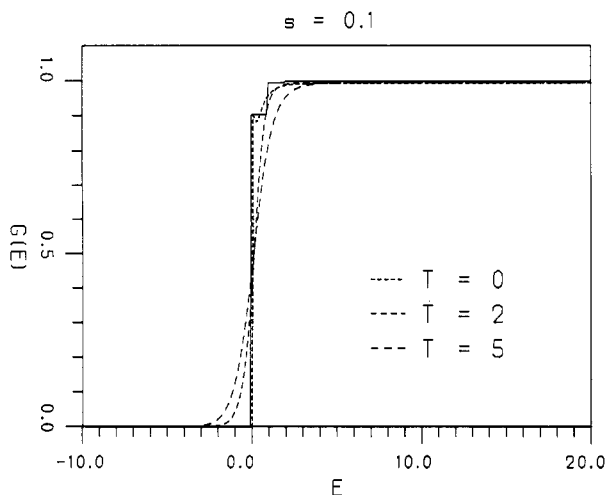


Figure 1. PITS spectra, $S = 0.1$. Smooth curves are obtained from the saddle-point method.

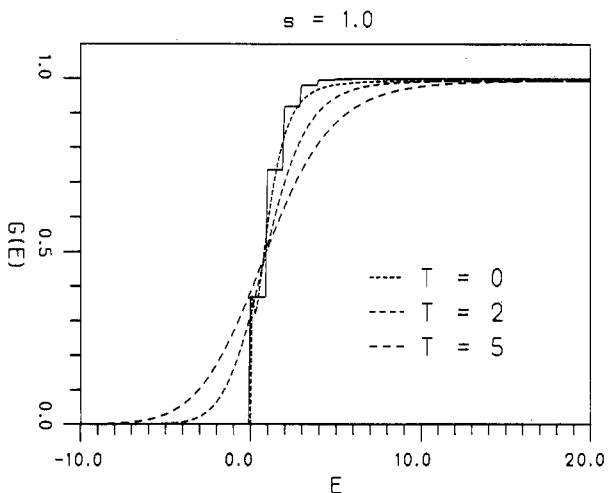


Figure 2. PITS spectra, $S = 1.0$. Smooth curves are obtained from the saddle-point method.

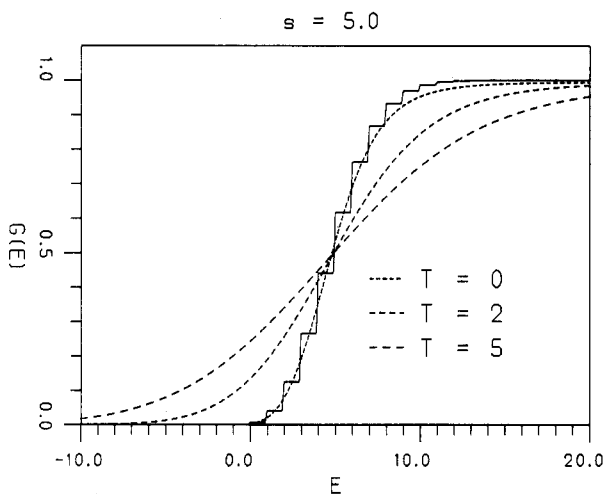


Figure 3. PITS spectra, $S = 5.0$. Smooth curves are obtained from the saddle-point method.

ionization energy accurately. The fitting of a PITS spectrum with the theoretical $G(E)$ can provide the additional information about the frequencies and normal coordinate displacements (through S) of the low-frequency modes. From Figures 1–4 we can see that the effect of temperature is to cause the red-shift of the apparent ionization threshold.

Recently it has been reported that hydrogen-bonding systems, dimers, trimers, etc. of aromatic molecules and some van der Waals molecules exhibit a long tail in PITS.^{9–13} However, it should

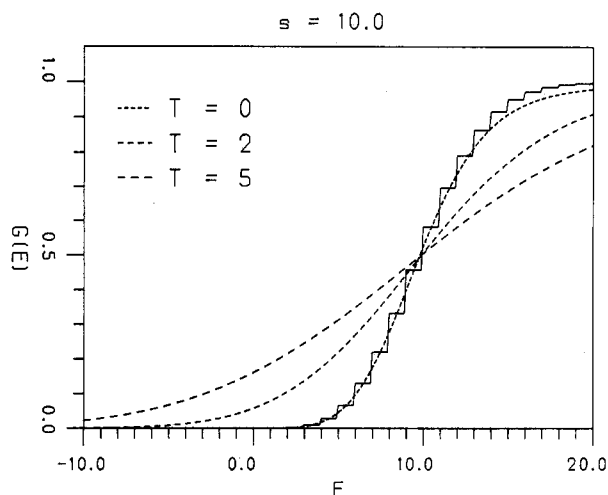


Figure 4. PITS spectra, $S = 10$. Smooth curves are obtained from the saddle-point method.

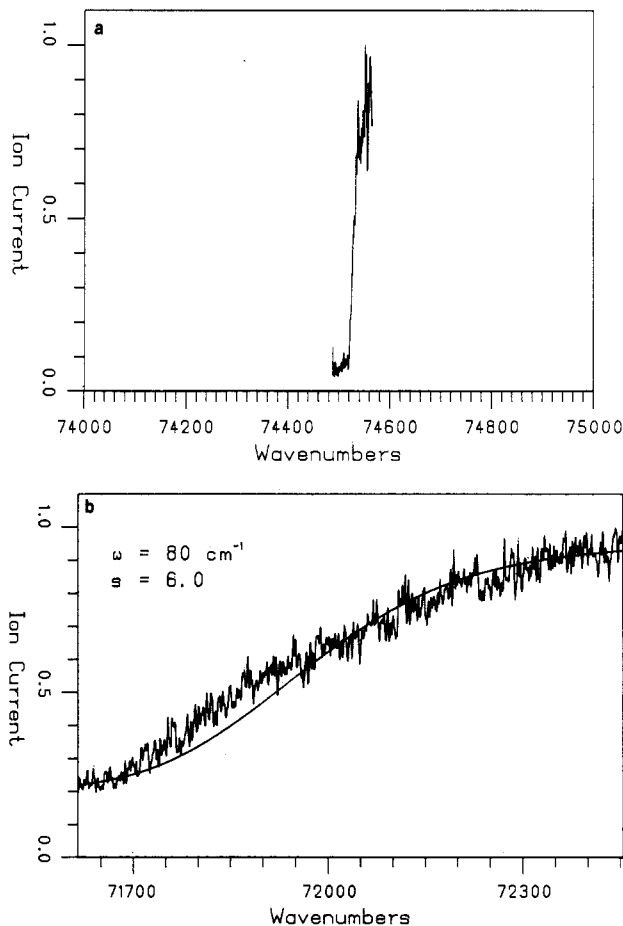


Figure 5. Photoionization threshold spectra of benzene and benzene dimer (6_0^1): (a) benzene; (b) benzene dimer (6_0^1).

be noted that part of this tail has to be attributed to the effect of electric field which has been used to repel ions. Very recently we have succeeded in measuring the PITS of molecules and clusters in field-free condition. This means that there is no electric field between the repelling plate and extracting plate in the ionization region during laser excitation and that after some hundred nanoseconds a fast electric pulse is applied to extract the ions formed into the TOF-MS. The experimental details and additional experimental results will be reported elsewhere.²¹ In Figure 5 we show the PITS of $(\text{benzene})_2$ by two-color photoionization excited to 6_0^1 of the excited electronic state of benzene. To see the dramatic long tail in the PITS of $(\text{benzene})_2$ we show the corresponding PITS of benzene monomer in Figure 5. By fitting the PITS of $(\text{benzene})_2$ with (2-15) (see Figure 5), we obtain $S = 6.0$, $\omega =$

80 cm⁻¹, and $I = 71\,504 \pm 30$ cm⁻¹. Using the reduced mass of (benzene)₂ and assuming that only one mode is responsible for S , we can estimate the intermolecular distance change as $\Delta r = -0.36$ Å. The resolution of the experiment does not warrant a fitting with a more sophisticated model presented in the previous sections. A main point here is that the fitting of PITS to a theoretical model can provide a more accurate determination of ionization energy and the additional information of the structure and vibrational frequencies of the cluster.

The effective distance change $\Delta r = -0.36$ Å between (benzene)₂ and (benzene)₂⁺ is quite reasonable. Recently, Jortner, Even, and Leutwyler²² have calculated the distance changes between (benzene-R) and (benzene-R)⁺ for R = Ne, Ar, Kr, and Xe. They found that Δr ranges from -0.12 Å for the benzene-Ne system to -0.33 Å for Xe. A somewhat bigger distance change for the (benzene)₂ system is expected because of the additional resonance charge-transfer interaction in (benzene)₂⁺. The intermolecular frequency of 80 cm⁻¹ is comparable with other weak complex systems like benzene-R (where R = Ne, Ar, Kr, Xe),²² carbazole-B (where B = H₂O, D₂O, NH₃,²³ and perylene-R (where R = Ne, Ar, Kr, Xe).²⁴

It should be noted that in this paper that we have only employed the first-order approximation of the saddle-point method which is accurate enough in most cases. However, if a better accuracy is desired, the second-order approximation can be used. Applications of the second-order approximation of the saddle-point method to photophysical processes can be found in the literature.¹⁸

In a two-color MPI experiment, the first laser is employed to excite the molecule to a specific vibronic level (or rovibronic level) in its first excited electronic state (i.e., resonance intermediate level) and the second laser is to promote the excited molecule into the ionization continuum. If the molecule is in the collision-free condition and if the intramolecular vibrational relaxation (IVR) is not fast (or does not take place), then we observe the single vibronic (or rovibronic) level photoionization threshold spectroscopy (see section 2B). If, on the other hand, the IVR is fast so that the intramolecular vibrational equilibrium is established, then we observe the so-called microcanonical PITS.¹⁸ In this case, we have

$$G(E, \epsilon) = \frac{2\pi}{\hbar} |D_{ki}|^2 \sum_v \sum_{v'} P_{iv}(\epsilon) |\langle v | v' \rangle|^2 H(E - I - E_{v'} + E_v) \quad (4-5)$$

where $P_{iv}(\epsilon)$ represents the microcanonical distribution function¹⁸

$$P_{iv}(\epsilon) = \frac{\delta(\epsilon - E_v)}{\rho(\epsilon)} \quad (4-6)$$

Here $\rho(\epsilon)$ denotes the density of states. Again we can apply the Laplace transformation and use the integral representation for the δ function to rewrite (4-5) as

$$L[G(E, \epsilon)] = \frac{2\pi}{\beta \hbar \rho(\epsilon)} |D_{ki}|^2 \frac{1}{2\pi i} \int_c d\beta_1 e^{\beta_1 \epsilon} \sum_v \sum_{v'} \exp[-\beta_1 E_v - \beta(I + E_{v'} - E_v)] |\langle v | v' \rangle|^2 \quad (4-7)$$

By using (2-8), (4-7) becomes

$$L[G(E_1 \epsilon)] = \frac{1}{\rho(\epsilon)} \frac{1}{2\pi i} \int_c d\beta_1 e^{\beta_1 \epsilon} L[Q(\beta_1)G(E)] \quad (4-8)$$

where $Q(\beta_1)$ represents the partition function of the molecule with the inverse temperature β_1 . As can be seen from (3-8), the microcanonical PITS is closely related to the thermal (or canonical) PITS, so the results for the microcanonical PITS will not be presented here.

In conclusion, in this paper, we have shown how to analyze the photoionization threshold spectra to obtain the information about

the intermolecular frequency and structure change and to determine the ionization potential more accurately; using the method presented in this paper it is possible to determine the ionization potential of van der Waals complexes, hydrogen-bonding systems, and other clusters to an accuracy on the order of 10 cm⁻¹. Although in this paper we have only treated the case in which the Condon approximation holds, for the case where the vibronic interaction is important, we have only to include the Franck-Condon factor of the type $|\langle v_i | Q_i | v_j \rangle|^2$ in $G(E)$ or $G_v(E)$, where Q_i is the so-called inducing (or promoting) mode, but due to the fact that the Q_i mode is usually of a relatively high frequency intramolecular mode, the effect of $|\langle v_i | Q_i | v_j \rangle|^2$ on PITS is usually not very important.

As the resolution of the photoionization experiments improves, it may become possible to resolve the fine structures in PITS or in the threshold region of photoelectron spectroscopy. Although we have treated PITS in this paper, one can apply the same type of theoretical treatment to study the ionization threshold spectroscopy of photoelectron experiments.

Acknowledgment. This work was supported by NSF and DFG. S.H.L. thanks Professor Hofacker for his gracious hospitality.

Appendix A

In this appendix we are concerned with the calculation of $F_j(\beta)$ defined by (2-10). Notice that it can be rewritten as

$$F_j(\beta) = \left(2 \sinh \frac{\hbar \omega_j}{2kT} \right) \sum_{v_j} \sum_{v'_j} \exp(\beta' E_{v_j} - \beta E_{v'_j}) |\langle v_j | v'_j \rangle|^2 \quad (A-1)$$

where $\beta' = 1/kT - \beta$. Writing the Franck-Condon factor $|\langle v_j | v'_j \rangle|^2$ in terms of a double integral

$$F_j(\beta) = \left(2 \sinh \frac{\hbar \omega_j}{2kT} \right) \sum_{v_j} \sum_{v'_j} \exp(-\beta' E_{v_j}) \times \exp(-\beta E_{v'_j}) \int_{-\infty}^{\infty} \int dQ_j d\bar{Q}_j X_{v_j}(Q_j) X_{v_j}(\bar{Q}_j) X_{v'_j}(Q'_j) X_{v'_j}(\bar{Q}'_j) \quad (A-2)$$

where X_{v_j} and $X_{v'_j}$ represent the vibrational wave functions. For a harmonic oscillator we can apply the Slater sum to (A-2) to carry out the summations over v_j and v'_j ; we obtain²⁰

$$F_j(\beta) = \left(2\beta_j \beta'_j \sinh \frac{\hbar \omega_j}{2kT} \right) \times \exp \left[- \frac{\beta_j^2 \beta'^2 \Delta Q_j^2}{\beta_j^2 \coth \frac{\beta \hbar \omega_j}{2} + \beta'^2 \coth \frac{\beta' \hbar \omega_j}{2}} \right] \left[(\sinh \beta' \hbar \omega_j \times \sinh \beta \hbar \omega_j) \left(\beta_j^2 \coth \frac{\beta' \hbar \omega_j}{2} + \beta'^2 \coth \frac{\beta \hbar \omega_j}{2} \right) \left(\beta_j^2 \tanh \frac{\beta' \hbar \omega_j}{2} + \beta'^2 \tanh \frac{\beta \hbar \omega_j}{2} \right) \right]^{-1/2} \quad (A-3)$$

where $\beta_j = (\omega_j/\hbar)^{1/2}$ and ΔQ_j represents the normal coordinate displacement.

For the displaced oscillator, we have $\Delta Q_j \neq 0$ and $\omega_j = \omega'_j$ (or $\beta_j = \beta'_j$). Equation A-3 reduces to (2-12). In (2-12), $S_j = (1/2)\beta_j^2 \Delta Q_j^2$. For the distorted oscillator, we have $\Delta Q_j = 0$ and $\omega_j \neq \omega'_j$. In this case (A-3) can be simplified as

$$F_j(\beta) = \frac{(1 - \rho_j)^{1/2}}{\left[\left(1 - \frac{\rho_j}{2} \right)^2 - \frac{\rho_j^2}{4} \operatorname{csch}^2 \frac{\hbar \omega_j}{2kT} \sinh^2 \frac{(\beta - \beta') \hbar \omega_j}{2} \right]^{1/2}} \quad (A-4)$$

(21) The details of the experimental method and other experimental results will be published separately.

(22) Jortner, J.; Even, W.; Leutwyler, S. *J. Chem. Phys.* **1983**, *78*, 309.

(23) Honegger, E.; Bombach, R.; Leutwyler, S. *J. Chem. Phys.* **1986**, *85*, 1234.

(24) Leutwyler, S. *J. Chem. Phys.* **1984**, *81*, 5480.

where $\omega_j' = \omega_j(1 - \rho_j)$.

Appendix B

In this appendix we show the calculation of $F_{v_j}(\beta)$ defined by (2-21). For a harmonic oscillator, we write the Franck-Condon factor in the double integral form and apply the Slater sum. The result is given by

$$F_{v_j}(\beta) = \frac{\beta_j'}{(2\pi \sinh \beta_j' \hbar \omega_j')^{1/2}} \int_{-\infty}^{\infty} \int dQ_j d\bar{Q}_j X_{v_j}(Q_j) X_{v_j}(\bar{Q}_j) \times \exp \left[-\frac{\beta_j'^2}{4} \left\{ (Q_j' + \bar{Q}_j')^2 \tanh \frac{\beta_j' \hbar \omega_j'}{2} + (Q_j' - \bar{Q}_j')^2 \coth \frac{\beta_j' \hbar \omega_j'}{2} \right\} \right] \quad (\text{B-1})$$

Using the contour-integral representation for the wavefunction $X_{v_j}(Q_j)$

$$X_{v_j}(Q_j) = N_{v_j} e^{-1/2\beta_j^2 Q_j^2} (-1)^{v_j} \frac{v_j!}{2\pi i} \int_c \frac{dz}{z^{v_j+1}} \exp(-z^2 - 2z\beta_j Q_j) \quad (\text{B-2})$$

where N_{v_j} is the normalization constant, we can carry out the integrals for Q_j and \bar{Q}_j in (B-1). The resulting expression for $F_{v_j}(\beta)$ is given by

$$F_{v_j}(\beta) = \left[2\pi\beta_j'^2 / \left[\left(\beta_j'^2 \cosh \frac{\beta_j' \hbar \omega_j'}{2} + \beta_j'^2 \sinh \frac{\beta_j' \hbar \omega_j'}{2} \right) \times \left(\beta_j'^2 \sinh \frac{\beta_j' \hbar \omega_j'}{2} + \beta_j'^2 \cosh \frac{\beta_j' \hbar \omega_j'}{2} \right) \right]^{1/2} \right] N_{v_j}^2 \left(\frac{v_j!}{2\pi i} \right)^2 \times \int_c \frac{dz_1}{z_1^{v_j+1}} e^{-a_j z_1^2 - 2b_j z_1} \int_c \frac{dz_2}{z_2^{v_j+1}} e^{-a_j z_2^2 - 2b_j z_2} \times \exp \left[c_j z_1 z_2 - \frac{\beta_j^2 \beta_j'^2 \Delta Q_j^2 \sinh \frac{\beta_j \hbar \omega_j'}{2}}{\left(\beta_j^2 \cosh \frac{\beta_j \hbar \omega_j'}{2} + \beta_j'^2 \sinh \frac{\beta_j \hbar \omega_j'}{2} \right)} \right] \quad (\text{B-3})$$

where

$$a_j = \frac{(\beta_j'^4 - \beta_j^4) \tanh \frac{\beta_j \hbar \omega_j'}{2}}{\left(\beta_j^2 + \beta_j'^2 \tanh \frac{\beta_j \hbar \omega_j'}{2} \right) \left(\beta_j^2 + \beta_j'^2 \coth \frac{\beta_j \hbar \omega_j'}{2} \right)} \quad (\text{B-4})$$

$$b_j = -\frac{\beta_j \beta_j'^2 \Delta Q_j \tanh \frac{\beta_j \hbar \omega_j'}{2}}{\left(\beta_j^2 + \beta_j'^2 \tanh \frac{\beta_j \hbar \omega_j'}{2} \right)} \quad (\text{B-5})$$

and

$$c_j = \frac{2\beta_j^2 \beta_j'^2 \left(\coth \frac{\beta_j \hbar \omega_j'}{2} - \tanh \frac{\beta_j \hbar \omega_j'}{2} \right)}{\left(\beta_j^2 + \beta_j'^2 \tanh \frac{\beta_j \hbar \omega_j'}{2} \right) \left(\beta_j^2 + \beta_j'^2 \coth \frac{\beta_j \hbar \omega_j'}{2} \right)} \quad (\text{B-6})$$

Expanding $\exp(c_j z_1 z_2)$ in (B-3) in power series, we can perform the double integrals to yield

$$F_{v_j}(\beta) = \left[\beta_j^2 \beta_j'^2 / \left[\left(\beta_j^2 \cosh \frac{\beta_j \hbar \omega_j'}{2} + \beta_j'^2 \sinh \frac{\beta_j \hbar \omega_j'}{2} \right) \times \left(\beta_j^2 \sinh \frac{\beta_j \hbar \omega_j'}{2} + \beta_j'^2 \cosh \frac{\beta_j \hbar \omega_j'}{2} \right) \right]^{1/2} \right] \times \exp \left[-\frac{\beta_j^2 \beta_j'^2 \Delta Q_j^2 \sinh \frac{\beta_j \hbar \omega_j'}{2}}{\left(\beta_j^2 \cosh \frac{\beta_j \hbar \omega_j'}{2} + \beta_j'^2 \sinh \frac{\beta_j \hbar \omega_j'}{2} \right)} \right] \times \sum_{n_j=0}^{v_j} \frac{(v_j!)}{n_j!} \left(\frac{c_j}{2a_j} \right)^{n_j} \left(\frac{a_j}{2} \right)^{v_j-n_j} H_{v_j-n_j} \left(\frac{2b_j}{a_j^{1/2}} \right)^2 \quad (\text{B-7})$$

where $H_{v_j-n_j}(x)$ represents the Hermite polynomial. For the displaced oscillator, we set $\beta_j = \beta_j'$ in (B-7) and obtain (2-22). On the other hand, for the distorted oscillator we set $\Delta Q_j = 0$ and we find

$$F_{v_j}(\beta) = \left[\beta_j^2 \beta_j'^2 / \left[\left(\beta_j^2 \cosh \frac{\beta_j \hbar \omega_j'}{2} + \beta_j'^2 \sinh \frac{\beta_j \hbar \omega_j'}{2} \right) \times \left(\beta_j^2 \sinh \frac{\beta_j \hbar \omega_j'}{2} + \beta_j'^2 \cosh \frac{\beta_j \hbar \omega_j'}{2} \right) \right]^{1/2} \right] \times \sum_{n_j=0}^{v_j} \frac{(v_j!)}{n_j!} \left(\frac{c_j}{2a_j} \right)^{n_j} \left(\frac{a_j}{2} \right)^{v_j-n_j} H_{v_j-n_j}(0)^2 \quad (\text{B-8})$$

Registry No. Benzene, 71-43-2; (benzene)₂, 6842-25-7.